LWT - Food Science and Technology 209 (2024) 116752

Contents lists available at ScienceDirect

LWT

journal homepage: www.elsevier.com/locate/lwt

# Authentication of premium Asian rice varieties: Stable isotope ratios and multi-elemental content for the identification of geographic fingerprints

Zoe Giannioti [a,b], Federico Ivan Brigante [a,c], Simon Kelly [d], Nives Ogrinc [e], Marta Jagodic Hudobivnik [e], Darja Mazej [e], Agostino Tonon [a], Luca Ziller [a], Chunyapuk Kukusamude [f], Supalak Kongsri [f], Saw Thantar [g], Henni Widyastuti [h], Yuwei Yuan [i], Luana Bontempo [a,c,*]

[a] Fondazione Edmund Mach, Via E. Mach 1, 38098, San Michele All'Adige, TN, Italy
[b] Centre for Agriculture, Food and Environment (C3A), University of Trento and Fondazione Edmund Mach Via E. Mach 1, 38098, San Michele All'Adige, TN, Italy
[c] Fondazione Edmund Mach, Fondazione OnFoods, Via Università N. 12, 43121, Parma, Italy
[d] Food Safety and Control Laboratory, Joint FAO/IAEA Centre of Nuclear Techniques in Food and Agriculture, Wagramer Strasse 5, PO Box 100, 1400, Vienna, Austria
[e] Department of Environmental Science, Jožef Stefan Institute, Jamova Cesta 39, Ljubljana, 1000, Slovenia
[f] Nuclear Technology Research and Development Center (NTRDC), Thailand Institute of Nuclear Technology (Public Organization), 9/9 Moo 7, Saimoon, Ongkharak, Nakhon Nayok, 26120, Thailand
[g] Department of Nuclear Technology, Technological University, Myopet Street, Kyaukse Township, Mandalay Division, Kyaukse, Myanmar
[h] National Research and Innovation Agency (BRIN), Research Organization for Nuclear Energy - Research Center for Radiation Processing Technology, B.J Habibie Science and Technology Park Building 720, Serpong, Indonesia
[i] Zhejiang Academy of Agricultural Sciences, 298 Desheng Middle Road, 310021, Hangzhou, Shangcheng, China

A R T I C L E I N F O

*Keywords:*
Food fraud
IRMS
ICP-MS
Data fusion
Multivariate analysis

A B S T R A C T

Over 90 percent of the world's rice is produced and consumed in the Asia-Pacific region. Varieties such as Thai Jasmine rice and Paw San (or "Myanmar pearl rice") are globally recognised as premium, while more local high-grade varieties include the Indonesian Ciherang and Inpari. Being able to trace the origin of these products has become necessary, since they are marketed at relatively higher prices compared to other cultivars, and they often become the target of fraudulent activities. In this work, we aimed to identify variables that could distinguish the premium-producing regions within each country, by Isotope Ratio Mass Spectrometry (IRMS) and Inductively Coupled Plasma- Mass Spectrometry (ICP-MS). Low-Level Data Fusion (LLDF) followed the analysis of more than 300 authentic samples, and (O)PLS-DA models yielded very high accuracy values. The most important geo-differentiating variables (VIP>1.4) were identified as: $\delta^{13}C$, $\delta^{18}O$, $\delta^{2}H$, $\delta^{34}S$, Co, Rb, Cu, Ba and Zn.

## 1. Introduction

Most of the world's rice production takes place in the Asia-Pacific region (Shahbandeh, 2024). Thai Hom Mali (or Jasmine) rice is one of the most popular rice varieties world-wide and, having also received the Geographical Indication (GI) recognition from the European Union, it is known for its high quality and unique characteristics (flavor, texture, and aroma) (EUIPO, 2019). Thai Hom Mali GI premium rice is produced in five provinces of the Thung Kula Rong-Hai area of northeastern Thailand, namely Roi Et, Mahasarakham, Surin, Yasothon, and Sisaket provinces.

Another premium aromatic rice is the Paw San, also known as "Myanmar pearl rice", which is characterized by elongation during cooking and a strong aroma (Oo et al., 2015). The highly photoperiod-sensitive varieties Paw San Bae Gyar and Paw San Hmwe are grown in Ayeyarwady delta regions (such as Pathein and Pyapone), while the higher priced and most valued, ShweBo Paw San, is grown in the Sagaing central dry region of the country (Aye, Khaing, Tun, Htun, & Win, 2019). Its harvest takes place once a year in the winter season from November to January, and its price can be up to three times higher than non-Paw San rice, also indicating the added value derived from its geographical origin (Thantar et al., 2024).

The increase of rice production has become the main objective of the Indonesian government's efforts to improve the economy (Sitaresmi,

* Corresponding author.
*E-mail address:* luana.bontempo@fmach.it (L. Bontempo).

https://doi.org/10.1016/j.lwt.2024.116752
Received 28 June 2024; Received in revised form 21 August 2024; Accepted 10 September 2024
Available online 11 September 2024

Hairmansis, et al., 2023). Significant diversity is noted amongst Indonesian rice species, with Ciherang variety being the most extensively grown after having successfully replaced the previously dominant IR64, and different Inpari varieties possessing characteristics such as high yields, resistance to pests and diseases, and good grain quality (Sitaresmi, Safitri, et al., 2023). Sixty percent of Indonesian rice production takes place in irrigated lowland environments, predominantly found in the northern part of Java Island (Sasmita & Nugraha, 2020). Previously tin-mined land is being changed into rice fields in the Bangka Belitung islands (Nurtjahya, Nur, & Mulyono, 2009), with continuous increase of upland rice cultivation and research focusing on crossing local Bangka rice with national varieties to achieve higher production rates and resistance to lodging (Mustikarini, Prayoga, Santi, & Sari, 2021).

Considering its high quality and production costs, Asian aromatic rice is sold at premium prices in the local and world market and is susceptible to economically motivated food frauds such as mislabelling or adulteration/substitution with less-costly cultivars (Cheajesadagul, Arnaudguilhem, Shiowatana, Siripinyanond, & Szpunar, 2013; Thantar et al., 2024). The institutional efforts to mitigate food fraud have led emerging research to focus on techniques and concepts that enhance the available traceability systems (Badia-Melis, Mishra, & Ruiz-García, 2015). Studies ascertain that consumers are willing to pay premium prices for food products with traceability certification labels; Boonkong, Jiang, Kassoh, and Srisukwatanachai (2023) revealed a positive preference and willingness to pay for the traceability attributes of rice by Chinese and Thai consumers, while Antriyandarti, Agustono, Ani, Rusdiyana, and Sukaton (2023) noted that Indonesian consumers preferred to buy local rather than imported rice in their consumer study.

Multi-elemental analysis by Inductively Coupled Plasma - Mass Spectrometry (ICP-MS) has been widely used in rice traceability studies (Li et al., 2022). In geographic authentication cases, ICP-MS provides insights into the geographical characteristics of the area of cultivation, as it reflects the bioavailable and mobilized nutrients of the underlying soil in the cultivation area (Bateman, Kelly, & Jickells, 2005). Recent works utilizing this technique have achieved the differentiation between Basmati and non-Basmati regions for Pakistani long grain rice (Arif et al., 2021), the distinction between rice samples from China, India, and Vietnam (Quinn et al., 2022), and the discrimination of rice produced in South Brazilian regions (Suchecki Barnet, Harumi Yamashita, Anzanello, & Pozebon, 2023). Parameters such as the geo-climatic factors, environmental conditions and cultivation practices have a decisive effect on isotopic fractionation processes, rendering Isotope Ratio Mass Spectrometry (IRMS) a valuable tool for food authentication studies (Sheng et al., 2022; Li et al., 2022). Rice geographic authentication has recently been achieved from the combination of the stable isotope ratios of $^{13}C/^{12}C$, $^{15}N/^{14}N$ and $^{18}O/^{16}O$ (expressed as $\delta^{13}C$, $\delta^{15}N$ and $\delta^{18}O$ values) for samples originating from different Asian countries (China, Thailand, Malaysia, Philippines and Pakistan) (Wang et al., 2020), while $\delta^{13}C$ and $\delta^{15}N$ values contributed to the regional discrimination of Pakistani basmati rice (Wadood et al., 2024).

Multi-elemental concentrations are often measured in conjunction with stable isotope ratios for a more nuanced assessment of geographic origin, considering the global variation of the 'light' bioelements and 'heavy' geoelements (Bateman et al., 2005). $\delta^{34}S$, Mn, and Mg were suggested as potential indicators of Asian rice, among 25 elements and 4 isotopes ($\delta^{13}C$, $\delta^{15}N$, $\delta^{18}O$ and $\delta^{34}S$), able to discriminate between six countries (Cambodia, China, Japan, Korea, Philippines and Thailand) (Chung et al., 2018).

Data Fusion (DF) is a novel statistical approach, preferred when dealing with complex data matrices. It finds applications in food authentication cases, since it can improve the classification results of a single technique (Callao & Ruisánchez, 2018). DF strategies are classified into low-level, mid-level, and high-level according to what information is fused. In Low-Level Data Fusion (LLDF), the raw data from different analytical techniques (represented by zeroth, first, or second order matrices) are the input of the DF workflow (Azcarate et al., 2021b). In this context, the application of DF requires handling multivariate datasets, thus utilizing multivariate data analysis or machine learning techniques either for exploratory or classification purposes (Smilde and Van Mechelen, 2019; Azcarate et al., 2021b).

In this work, we collected 340 authentic samples of different Asian rice varieties from premium and non-premium producing areas of Thailand, Myanmar, Indonesia, and China, with the aim to identify the most important variables of the premium samples of each country. The techniques used include ICP-MS for the analysis of 25 selected macro, micro and trace elements, and stable isotope ratio analysis (SIRA) by elemental analyser-isotope ratio mass spectrometry (EA-IRMS), using both combustion and thermochemical conversion techniques for the isotope ratios $^{13}C/^{12}C$, $^{15}N/^{14}N$, $^{34}S/^{32}S$, and $^{18}O/^{16}O$, $^{2}H/^{1}H$, respectively. Thereafter, we aimed to classify the rice samples based on their geographic origin integrating the isotopic and multi-elemental data in an LLDF approach. The results of this study contribute to the food traceability database of low-income countries and suggest reliable indicators for the authenticity of Asian varieties appreciated worldwide, such as Jasmine and Paw San rice.

## 2. Materials & methods

### 2.1. Sampling

The rice sampling sites in Thailand, Myanmar, China, and Indonesia are shown in Fig. 1. A total of 170 samples were collected from Thai Hom Mali rice producers in Thailand. These were collected in 2018 from Northeastern (Kalasin, Mukdahan, Yasothon, Amnat Charoen, Ubon Ratchathani, Surin, Roi Et, and Mahasarakham) and Northern (Phayao, Chiang Rai, and Chiang Mai) provinces, and in 2019 from Northeastern (Bueng Kan, Nakhon Phanom, Sakon Nakhon, Udon Thani, Nong Khai, Nong Bua Lam Phu, and Khon Kaen) and Northern (Phayao, Chiang Rai, and Chiang Mai) provinces. Eighty-seven Paw San rice samples were collected in 2020 from the Ayeyarwady Division (Pyapon, Bogalay, Dedaye, Kyaiklat, Pathein, and Myaungmya), and Shwebo District of Myanmar. Thirty-six rice samples were collected in 2017 from different regions of China: Heilongjiang (HLJ), Jilin (JL) and Liaoning (LN) in the northeast, Hubei (HB), Hunan (HN), Jiangxi (JX) and Anhui (AH) in the center, Guangxi (GZ) in the south, Zhejiang (ZJ) and Jiangsu (JS) in the southeast. Forty-six samples of Indonesian rice were collected between 2019 and 2022 in Java (Ciherang, Inpari, Basmati and Mokingga varieties) and Bangka Belitung (Balok, Mahadi, Mayang Pandan, Radin, Mat Merah varieties) Island Provinces.

### 2.2. Stable isotope ratio analysis

The samples were ground to a fine powder and weighed using a microbalance into tin (6 mg for $^{13}C/^{12}C$, $^{15}N/^{14}N$ and $^{34}S/^{32}S$) or silver capsules (0.2 mg for $^{2}H/^{1}H$ and $^{18}O/^{16}O$). For the analysis of $^{2}H/^{1}H$, the comparative equilibration method was used (Wassenaar & Hobson, 2003). Samples and standards were left in lab air moisture for at least 96 h and then placed in a desiccator with $P_2O_5$ under nitrogen atmosphere. Each sample was weighed and analysed in triplicate for C, N, S analysis and in duplicate for O and H.

The $^{13}C/^{12}C$, $^{15}N/^{14}N$ and $^{34}S/^{32}S$ ratios were measured simultaneously using an isotope ratio mass spectrometer (Elementar Analysensysteme GmbH, Langenselbold, Germany) after total combustion in an elemental analyser (Vario Isotope Cube; Elementar Analysensysteme GmbH). The $^{2}H/^{1}H$ and $^{18}O/^{16}O$ ratios were measured simultaneously using an isotope ratio mass spectrometer (Finnigan DELTA XP; Thermo Fisher Scientific, Waltham, MA, USA) coupled with a pyrolyzer (Finnigan DELTA TC/EA, high temperature conversion elemental analyser, Thermo Scientific). The instrumental conditions were as described in Campanelli et al. (2024).

The isotope ratios were expressed in $\delta$ ‰ in relation to the


**Fig. 1.** Map of sampling locations.

international standard V-PDB (Vienna-Pee Dee Belemnite) for $\delta^{13}$C, V-SMOW (Vienna-Standard Mean Ocean Water) for $\delta^{2}$H and $\delta^{18}$O, V-CDT (Vienna Canyon Diablo Troilite) for $\delta^{34}$S and Air (atmospheric $N_2$) for $\delta^{15}$N, according to the equation below, where R is the ratio of the heavy ($^{i}$E) to light ($^{j}$E) isotope of an element E:

$$\delta^{i}\left(E_{sample/standard}\right) = \frac{R\left({}^{i}E/{}^{j}E\right)_{sample}}{R\left({}^{i}E/{}^{j}E\right)_{standard}} - 1$$

International reference materials (U.S. Geological Survey), and an in-house working standard (wheat flour), were used to normalise the values, namely, USGS90 (Millet flour, $\delta^{15}$N: 8.84‰, $\delta^{13}$C: −13.75‰, $\delta^{34}$S: −15.14‰) and USGS88 (collagen, $\delta^{15}$N: 14.96‰, $\delta^{13}$C: −16.06‰, $\delta^{34}$S: 17.1‰) for N, C, S, and USGS90 (millet flour, $\delta^{2}$H: −13.9‰, $\delta^{18}$O: 35.9‰), USGS91 (rice flour, $\delta^{2}$H: −45.7‰, $\delta^{18}$O: 21.13‰) for H, O.

### 2.3. Multi-elemental analysis

#### 2.3.1. Sample digestion

The rice samples (0.20 g) were weighed into Teflon vials, mixed with 1 mL of concentrated $HNO_3$ (Suprapur, Carlo Erba, Italy) and digested in a microwave (UltraWAVE, Milestone, Italy) (20 min heating to 240 °C, 15 min hold at 240 °C). Reference materials and blanks were included in each run (every tenth sample). The reference materials were NIST (National Institute of Standards and Technology, USA) SRM 1568b Rice Flour and NIST SRM 8436 Durum Wheat Flour. After digestion the samples were diluted to 10 mL with Milli-Q water.

#### 2.3.2. ICP-MS analysis

Measurement of 25 elements (Na, Mg, Al, P, S, K, Ca, V, Cr, Mn, Fe, Co, Ni, Cu, Zn, As, Se, Rb, Sr, Mo, Cd, Sn, Ba, Hg, and Pb) in rice digests was performed by ICP-MS (Agilent ICP-QQQ 8800, California, USA), equipped with an Octapole Reaction System (ORS). Instrumental conditions were as follows: Scott-type spray chamber, MicroMist; spray chamber temperature: 2 °C; plasma gas flow rate: 15 L $min^{-1}$; carrier gas flow rate: 0.95 L $min^{-1}$; make-up gas flow rate: 0.1 L $min^{-1}$; sample solution uptake flow rate, 1 mL $min^{-1}$; RF power 1550 W; reaction cell gas: helium, oxygen, or hydrogen. Tuning of the instrument was performed daily using a solution containing Li, Mg, Y, Ca, Tl and Co. Limits of detection (LOD) (Table A1), calculated as three times the standard deviation of blanks, were below the elemental concentrations encountered in the rice digests. Certified reference materials (CRMs) used are included in Table A1.

### 2.4. Statistical analysis

All statistical analyses and graph designs were carried out in R Studio (R Studio team, 2023).

#### 2.4.1. Low-Level Data Fusion (LLDF) of IRMS and ICP-MS data

The zeroth-order data blocks (Mx1 column vectors where M is the total number of samples) coming from IRMS (MxN where N is the number of isotopes) and multi-elemental analysis (MxK where K is the number of elements) were divided into training and validation test sets separately before LLDF. Then, the data blocks were concatenated horizontally to create the fused matrix of MxQ dimensions where Q is the sum of N and K. The concatenated data were autoscaled prior to application of multivariate models. (Orthogonal) Partial Least Squares - Discriminant Analysis or (O)PLS-DA models were built for the three fused data matrices with training sets containing an 80% of the total number of rice samples. These classification models aim to find a division of the space into two regions, one for each class. In the orthogonal extension of the method, the predictive (correlated to Y) and orthogonal (uncorrelated to Y) variations of the X block are modeled separately, thus simplifying interpretation, and improving predictive performance. In cases of two-class separation where the orthogonal variation was not significant for the model, PLS-DA was performed, so for simplicity the mention of (O)PLS-DA was adopted. For each (O)PLS-DA model, a permutation test was performed to evaluate the significance and potential overfitting. The chance that the current model is not statistically improved by random permutation of the Y-block is measured by calculating R2Y (goodness of fit) and Q2Y (predictability) of the random permutations. The root mean squared error of estimation (RMSEE) was calculated for each model. K-fold cross-validation was applied to the models ($k = 7$) and R2X (explained variance of the X-block), R2Y and Q2Y were measured for the training set. The total inertia of the models (this is, the resistance to fluctuations in the data) explained by the selected components was plotted. Outlier diagnostics plots were obtained for each model to evaluate the presence of outliers (Hubert, Rousseeuw, & Vanden Branden, 2005). Confusion matrices were obtained for each of the test sets and the classification accuracy was measured based on the number of correctly classified samples by each model. Variable selection was carried out by means of variable importance in projection scores (VIP). However, it has been demonstrated in the case of OPLS modeling that the VIP remains intact irregardless of the number of orthogonal components selected by the models (Galindo-Prieto, Eriksson, & Trygg, 2014; Thévenot et al., 2015). So, a new VIP measure of the predictive and orthogonal components was proposed. The predictive component of the VIP score (VIP_pred) was obtained for OPLS models (Galindo-Prieto et al., 2014). The variables with a VIP score (either VIP or VIP_pred) higher than 1 were selected as discriminant of the Asian rice varieties.

## 3. Results & discussion

### 3.1. Stable isotopes

The results of the IRMS analysis for the different countries are summarized in Table 1. Significant differences ($p < 0.05$) were found between all countries for $\delta^{13}C$, with the lowest values noted in Indonesia and the highest in Thailand. Considering that the main determining factor for $\delta^{13}C$ in plants is the photosynthetic pathway (C3, CAM or C4), and that rice is a C3 plant, the values measured were within the expected C3 range (−21 ‰ to −35 ‰) (Islam & Khan, 2019). The effect of variety on $\delta^{13}C$ values of plants has been found to be insignificant (Anderson & Smith, 2006), therefore, discrimination between different varieties can be indirectly attempted by discrimination between the premium and non-premium producing regions. Climatic factors including humidity, sunshine and temperature also affect $\delta^{13}C$ values, with plants in warm and humid environments exhibiting lower $^{13}C/^{12}C$ ratios compared to those in cooler and drier conditions, since they exhibit higher stomatal opening, increased uptake of $CO_2$ and enrichment of the plant tissues in $^{12}C$ due to the preferential uptake of the lighter isotope ($^{12}C$) relative to the heavier isotope ($^{13}C$) during photosynthesis (Camin et al., 2007). Moreover, higher altitudes, and lower levels of atmospheric $CO_2$, are associated with higher $\delta^{13}C$ due to the carboxylation effect which results in decreased fractionation of the carbon isotopes and smaller differences in $\delta^{13}C$ between atmospheric $CO_2$ and plant tissues (Körner, Farquhar, & Roksandic, 1988). Generally, the regions included in this study such as Bangka Belitung (Indonesia), Shwe Bo and Ayeyarwady (Myanmar), as well as most of the Chinese regions are low-lying, without particularly high altitudes. However, significant difference was observed between the $\delta^{13}C$ values of South (GZ) and Northeast (HLJ, JL, LN) Chinese regions (Figure A1), since the first exhibits a subtropical climate with high temperatures and heavy rainfall and the latter have a temperate continental climate. Furthermore, discrimination was achieved between the Northern and Northeastern (premium) regions of Thailand for both 2018 and 2019 (Fig. 2) due to their geoclimatic differences. Specifically, while both can experience hot and humid conditions, Northern Thailand mostly exhibits cooler temperatures and lower humidity compared to the Northeastern part of the country and can exhibit higher altitudes than the latter. Kukusamude and Kongsri (2018) reported $\delta^{13}C$ values which ranged between −27.8 and −26.3 ‰ for Thai Jasmine rice produced in the Northeastern (including Yasothon, Roi Et, Surin, Sisaket, and Mahasarakham provinces), in agreement with our findings for the same provinces (total range −27.5 to −26.3 ‰). Moreover, Wang et al. (2020) reported $\delta^{13}C$ values of $-27.3 \pm 0.6$ ‰ for Thai rice samples, as well as ranges from $-28.2 \pm 0.5$ ‰ to $-26.8 \pm 0.4$ ‰ for Chinese rice, with similar findings noted in literature for the latter (Li et al., 2022; Li et al., 2021).

On the other hand, $\delta^{15}N$ values are mainly affected by agricultural practices, soil nutrients and fertilizer application (Bateman et al., 2005). No significant differences were seen between the four countries studied, except for Myanmar (Table 1), which had the lowest average value (1.9 ‰) compared to averages of greater than 4 ‰ for the other countries. This may be attributed to the low nitrogen tolerance of Paw San variety (Thein, 2015), which exhibits high N use efficiency and selectively uptakes N from natural sources and fertilizers, leading to lower $\delta^{15}N$ values in its tissues compared to other varieties. Moreover, higher $\delta^{15}N$ values were noted in ShweBo Paw San compared to Ayeyarwady (Fig. 3), which could be attributed to the reduced application of both organic and conventional fertilizers in the latter compared to the Sagaing region (Myint & Napasintuwong, 2015).

Wide $\delta^{34}S$ ranges have been reported in literature for plants (from −30

**Table 1**
Rice stable isotope values from the different countries of origin. Results expressed as mean, minimum and maximum of the measured values (‰).

| δ (‰) | Thailand | | | Myanmar | | | China | | | Indonesia | | |
|---|---|---|---|---|---|---|---|---|---|---|---|---|
| | Mean | min | max | Mean | min | max | Mean | min | max | Mean | min | max |
| C | −26.8 | −28.1 | −25.1 | −27.2 | −28.0 | −25.8 | −27.6 | −29.0 | −25.9 | −28.4 | −29.4 | −27.2 |
| N | 4.5 | 1.3 | 10.2 | 1.9 | 0.1 | 4.5 | 4.3 | 2.3 | 6.5 | 4.5 | 1.9 | 8.8 |
| S | 2.8 | −9.0 | 10.2 | 10.9 | −4.1 | 21.6 | 2.7 | −6.2 | 8.6 | 2.2 | −5.2 | 7.7 |
| O | 27.5 | 22.6 | 31.4 | 25.1 | 21.7 | 29.9 | 22.3 | 17.5 | 27.1 | 23.2 | 19.7 | 28.4 |
| H | −42 | −58 | −24 | −42 | −57 | −29 | −53 | −70 | −23 | −47 | −62 | −31 |

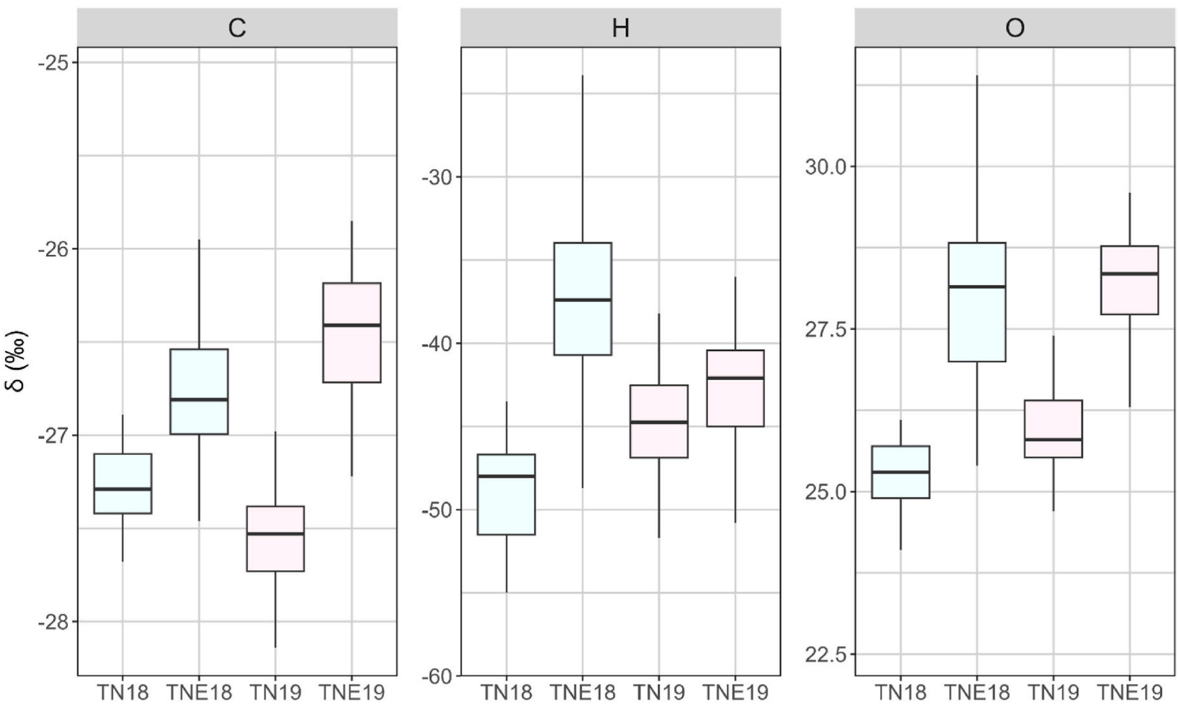


**Fig. 2.** Discrimination between Jasmine rice from the North and Northeast of Thai regions for the years 2018 and 2019 (TN18, TNE18, TN19, TNE19) based on $\delta^{13}$C, $\delta^{2}$H and $\delta^{18}$O values. Northeast includes the premium-grade GI Jasmine rice regions of Roi Et, Mahasarakham, Surin, and Yasothon.

to +35‰), since they depend on both the mobile sulphate in the soil and the atmospheric sulphate, with the first being influenced by factors including the composition of bedrock, the presence of organic matter and the degree of erosion, and the second being affected by the sea-spray effect, the occurrence of dimethyl sulphide (DMS), volcanic gas and anthropogenic sources (Rodiouchkina, Rodushkin, Goderis, & Vanhaecke, 2022). As seen in Table 1, the highest $\delta^{34}$S values were found in Myanmar rice, with an average of 10.9 ‰ against approximately 2–3 ‰ of Thailand, China, and Indonesia. Myanmar contains an abundance of coal sources, with mines along the Ayeyarwady river basin, which comprises one of the main coal production areas in the country (JICA, 2013). The release of sulphur-bearing minerals during extraction processes thus results in increased $\delta^{34}$S values, which also explains the elevated average of Ayeyarwady Paw San rice compared to the non-coal-producing ShweBo (Fig. 3). Moreover, Ayeyawardy region is near the sea and can therefore experience higher levels of sea spray contributing to the increase of $\delta^{34}$S values, since marine sources exhibit higher $\delta^{34}$S values compared to terrestrial (Rodiouchkina et al., 2022). The seaspray effect may also be responsible for the higher values noted in the SE coastal regions of China (ZJ and JS), while elevated $\delta^{34}$S values in NE and C may result from anthropogenic sulphur emissions since these areas have significant industrial activity, unlike GZ in the south which exhibited the lowest values (below 0 ‰) (Figure A1). Lastly, a difference of circa +5‰ was found between the means of the Indonesian regions of Java and Bangkla Belitung (Figure A2), which can be explained by the volcanic arc and soils found in the former (Philibosian & Simons, 2011).

Hydrogen and oxygen isotope ratios in rice are influenced by those of rainfall and irrigation water, with fractionation processes occurring throughout the water cycle and altering the relative isotope values (Liu et al., 2019). Higher $\delta^{2}$H and $\delta^{18}$O values are noted when evapotranspiration rates increase, because of the consequential increase in the loss of water molecules and the preferential loss of the lighter isotopologues of water, such as when going from cool to warm environments, from high to low altitudes, as well as upon decreasing inland distance from the coast (Li et al., 2022). The lowest $\delta^{2}$H and $\delta^{18}$O values among the countries examined herein were found in the Chinese rice samples (Table 1), ranging between −69.9 and −23.2 ‰ and 17.5–27.1 ‰, respectively. Other works have reported $\delta^{18}$O values in the same range (Chung et al., 2018), and noted the same increasing trend between the $\delta^{18}$O of rice samples from China, Myanmar, and Thailand (Li et al., 2015). Inter-country comparison revealed the highest values in the southeast Chinese regions (ZJ, JS) compared to inland areas (HLJ, JL, HN and GZ) (Wang et al., 2020; Liu et al., 2019). Similarly, $\delta^{2}$H values in the southeast (ZJ, JS) were the highest compared to the other regions (HLJ, JL, HN and GZ) (Liu et al., 2019), in agreement with our findings (Figure A1). Thai jasmine rice from northeastern regions (Yasothon, Roi Et, Surin, and Mahasarakham provinces) was found to exhibit $\delta^{18}$O values between 23.44 and 26.69 ‰ (Kukusamude & Kongsri, 2018), which are lower than our findings (Fig. 2). The yearly impact on the isotope ratios can be also seen in Fig. 2, and it can be attributed to the significant annual rainfall variation noted in the country (Chutsagulprom, Chaisee, Wongsaijai, Inkeaw, & Oonariya, 2022).

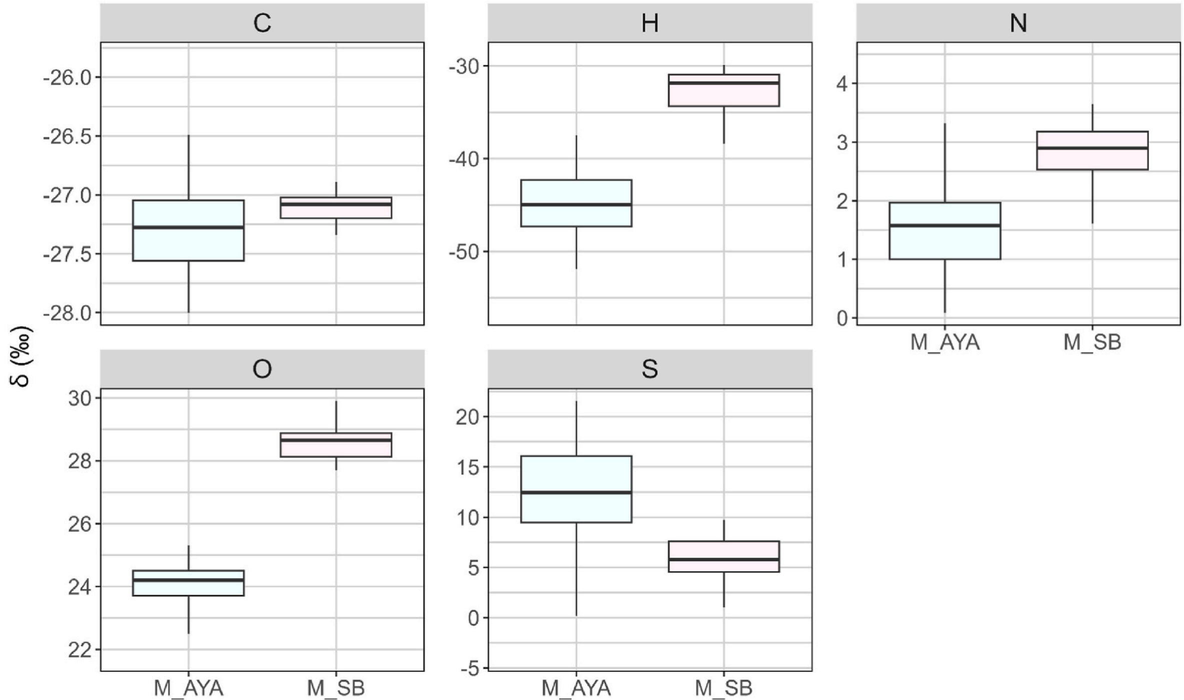


**Fig. 3.** Discrimination between Paw San rice from Ayeyarwady (M_AYA) division and Shwebo (M_SB) in Myanmar, based on $\delta^{13}$C, $\delta^{2}$H, $\delta^{15}$N, $\delta^{18}$O and $\delta^{34}$S values.

Cultivar type is an additional factor which was found to contribute significantly to the differences in $\delta^{2}$H and $\delta^{18}$O values between basmati and non-basmati varieties, with plant morphology (height and leaf type) and drought resistance influencing leaf water evaporation rates (Wadood et al., 2024). This could explain the wide range of values and the significant difference observed between the $\delta^{2}$H and $\delta^{18}$O values of white rice varieties (Ciherang, Inpari, Basmati) from Java and the brown rice varieties (Inpari, Balok, Mahadi) from Bangka Belitung (Figure A2).

Lastly, clear separation was seen between the $\delta^{2}$H and $\delta^{18}$O values of Paw San rice from ShweBo and Ayeyarwady in Myanmar (Fig. 3), which could be explained by the predominantly hotter and drier conditions of ShweBo compared to Ayeyarwady region, as well as the higher

**Table 2**
ICP-MS multi-elemental analysis results for the different countries reported as mean, minimum and maximum values measured (ng/g). They are summarized at the bottom of the table and grouped in macro-elements (Mg, P, S, K, Ca, Na), micro-elements (Al, V, Cr, Mn, Fe, Co, Ni, Cu, Zn, Mo, Se, Rb, Sr) and potentially toxic elements (As, Cd, Sn, Ba, Hg, Pb).

| ng/g | Thailand | | | Myanmar | | | China | | | Indonesia | | |
|---|---|---|---|---|---|---|---|---|---|---|---|---|
| | mean | min | max | mean | min | max | mean | min | max | mean | min | max |
| Na | 1869 | 669 | 12648 | 12463 | 2391 | 55544 | 3450 | 1397 | 9408 | 6260 | 1993 | 139680 |
| Mg | 398255 | 111124 | 688927 | 815592 | 246426 | 1497274 | 167598 | 54359 | 412249 | 332805 | 98260 | 1836188 |
| Al | 754 | 92 | 7676 | 8034 | 560 | 74645 | 1713 | 117 | 9392 | 5090 | 335 | 94960 |
| P | 1295257 | 594999 | 2007710 | 2387013 | 978848 | 4011415 | 799922 | 484157 | 1389237 | 1245247 | 664996 | 5282524 |
| S | 920246 | 666748 | 1315495 | 1176370 | 928785 | 1494996 | 932975 | 656520 | 1177669 | 1221177 | 866782 | 2727762 |
| K | 1053601 | 545375 | 1459938 | 1769467 | 755905 | 2888531 | 701129 | 411688 | 1058879 | 989062 | 411949 | 3558152 |
| Ca | 50585 | 32698 | 76759 | 63465 | 36176 | 114219 | 46518 | 35173 | 74812 | 56199 | 12752 | 187328 |
| V | 1 | 0.4 | 8 | 11 | 2 | 93 | 5 | 1 | 56 | 5 | 0.4 | 78 |
| Cr | 68 | 20 | 182 | 116 | 15 | 905 | 380 | 38 | 1239 | 32 | 6 | 133 |
| Mn | 11466 | 6992 | 22892 | 17149 | 5603 | 34476 | 8943 | 5523 | 14918 | 7683 | 1932 | 15741 |
| Fe | 3208 | 1527 | 6704 | 11053 | 2819 | 49073 | 6753 | 1353 | 38373 | 8019 | 1944 | 83328 |
| Co | 17 | 4 | 99 | 25 | 7 | 70 | 7 | 1 | 18 | 12 | 0.5 | 58 |
| Ni | 363 | 25 | 2413 | 893 | 166 | 2812 | 532 | 111 | 1341 | 272 | 17 | 1007 |
| Cu | 6387 | 273 | 49690 | 2388 | 655 | 4491 | 2161 | 1063 | 3502 | 2360 | 512 | 4863 |
| Zn | 19399 | 11088 | 27109 | 21603 | 11302 | 29967 | 11741 | 7231 | 17543 | 17420 | 5889 | 44349 |
| As | 111 | 29 | 321 | 112 | 30 | 316 | 96 | 46 | 148 | 37 | 1 | 203 |
| Se | 50 | 8 | 357 | 40 | 7 | 129 | 30 | 12 | 99 | 64 | 6 | 203 |
| Rb | 6560 | 840 | 37376 | 1797 | 368 | 7568 | 2021 | 298 | 8390 | 6305 | 478 | 19178 |
| Sr | 96 | 33 | 579 | 260 | 76 | 523 | 83 | 28 | 171 | 151 | 31 | 527 |
| Mo | 481 | 143 | 1345 | 296 | 171 | 658 | 472 | 219 | 993 | 408 | 66 | 1042 |
| Cd | 53 | 1 | 539 | 20 | 2 | 73 | 70 | 1 | 310 | 19 | 1 | 82 |
| Sn | 495 | 0.4 | 4448 | 16 | 2 | 152 | 4 | 1 | 13 | 8 | 1 | 29 |
| Ba | 260 | 21 | 1079 | 122 | 27 | 364 | 277 | 99 | 607 | 137 | 15 | 869 |
| Hg | 4 | 1 | 39 | 2 | 1 | 4 | 3 | 1 | 7 | 2 | 0.2 | 14 |
| Pb | 5 | 1 | 47 | 13 | 3 | 38 | 5 | 1 | 17 | 7 | 1 | 32 |
| Total, ng/g (sum of means) | Thailand | | | Myanmar | | | China | | | Indonesia | | |
| Macronutrients | 3,719,814 | | | 6,224,370 | | | 2,651,593 | | | 3,850,749 | | |
| Micronutrients/Trace elements | 48,851 | | | 63,663 | | | 34,842 | | | 47,820 | | |
| Potentially toxic | 926 | | | 284 | | | 456 | | | 210 | | |

precipitation levels noted in the latter, especially during monsoon season (Oo, Haishan, & Jonah, 2023).

### 3.2. Multi-elemental

The results of the ICP-MS analysis of the 25 elements are summarized for each country in Table 2, including the total sum of different elemental groups, i.e. macronutrients (required in large amounts by plants), micronutrients (required in small amounts but still essential) and potentially toxic elements. The concentrations of both macronutrients and micronutrients were the highest in Myanmar, being double the ones of Chinese samples, while Thailand exhibited similar concentrations with Indonesia, both being lower than Myanmar and higher than China. Traces of elements with increased toxicity risks were detected within the internationally accepted Codex maximum levels (MLs) for rice and cereals (200–350 ng/g for As, 400 ng/g for Cd, 200 ng/g for Pb) (Codex Alimentarius, 1995).

A preliminary inter-country comparison of the elemental content in the different regions can be seen in Fig. 4. The northeastern regions of Thailand, which include the premium Jasmine rice-producing Roi Et, Yasothon, Surin, among others, exhibited higher concentrations of Ba, Co, Cr, Cu, Ni, Pb, Rb, and Sn compared to the northern regions such as Phayao, Chiang Rai and Chiang Mai. Paw San rice samples from Ayeyarwady region of Myanmar exhibited higher values of Al, Ba, Ca, Fe, Hg, Mg, Sn, Sr and V compared to those from ShweBo, with the latter being more concentrated in Pb and Rb. Ciherang and Inpari samples from Java Island exhibited higher concentrations of Al, As, Cd, Co, and Hg than the Bangka Belitung varieties which were more concentrated in Ca, Ni, Pb, Se and Sn. Among the different areas in China, the southern samples (GZ) exhibited the highest concentrations of Al, Fe, Se and V. The lowest concentrations among all regions were those of Pb in the Northeast, while the highest concentrations of Cr, Hg and Na were found in the Southeastern. Central areas exhibited a similar profile to the NE, except for Pb which was lower and Mn which was higher in NE.

Such differences in the elemental compositions arise from the distinct climatic conditions and the characteristics of the soils influencing the availability and uptake of elements in the rice growing period (Zhao, Wang, & Yang, 2020). The soil pH conditions strongly impact the bioavailability of heavy metals (e.g. Al, Pb), which is higher in weakly-acidic soils than in weakly-alkaline soils, such as in the case of southern compared to northern China (Liu et al., 2019). The heavy dependance of Paw San rice cultivation on pesticides treatment, as well as on super phosphate ($P_2O_5$) fertilizer, which reaches triple levels on average between Ayeyarwady and ShweBo compared to non-Paw San cultivation (Myint & Napasintuwong, 2015), could result in an elemental profile higher in P and inorganic ions introduced from common fertilizers (e.g. $KNO_3$, $Ca(H_2PO_4)_2$) (Zhi, Yuan, Yudi et al., 2023). Moreover, soils of major rice-producing areas in Thailand and southern China were formed from river sediments naturally rich in trace elements, and thus require less fertilizer application compared to other areas in Asia, resulting in lower macro- but higher micro element concentrations (Zhi, Yuan, Yudi et al., 2023). Lastly, tin mining processes which prevailed in the Bangka Belitung Islands province have had significant effects in its soil characteristics, with studies noting low pH, lower available phosphate and exchangeable K (Wulandari, Agus, Rosita, Mansur, & Fikri Maulana, 2022), as well as elevated S levels released from the pyrite layers during excavations and the presence of micro- and toxic elements (Mn, Cu, Zn, Sn, Pb, Cd and Hg) (Sukarman, Gani, & Asmarhansyah, 2020), always within tolerable limits for rice.

### 3.3. Low-Level Data Fusion (LLDF) of IRMS and ICP-MS data

The results from the (O)PLS-DA models for the geographic discrimination of Myanmar, Thai, and Indonesian rice samples are presented in Figs. 5 and 6, and A3, respectively. For the case of Thai rice samples, the separation of samples in the first 2 latent variables did not allow the

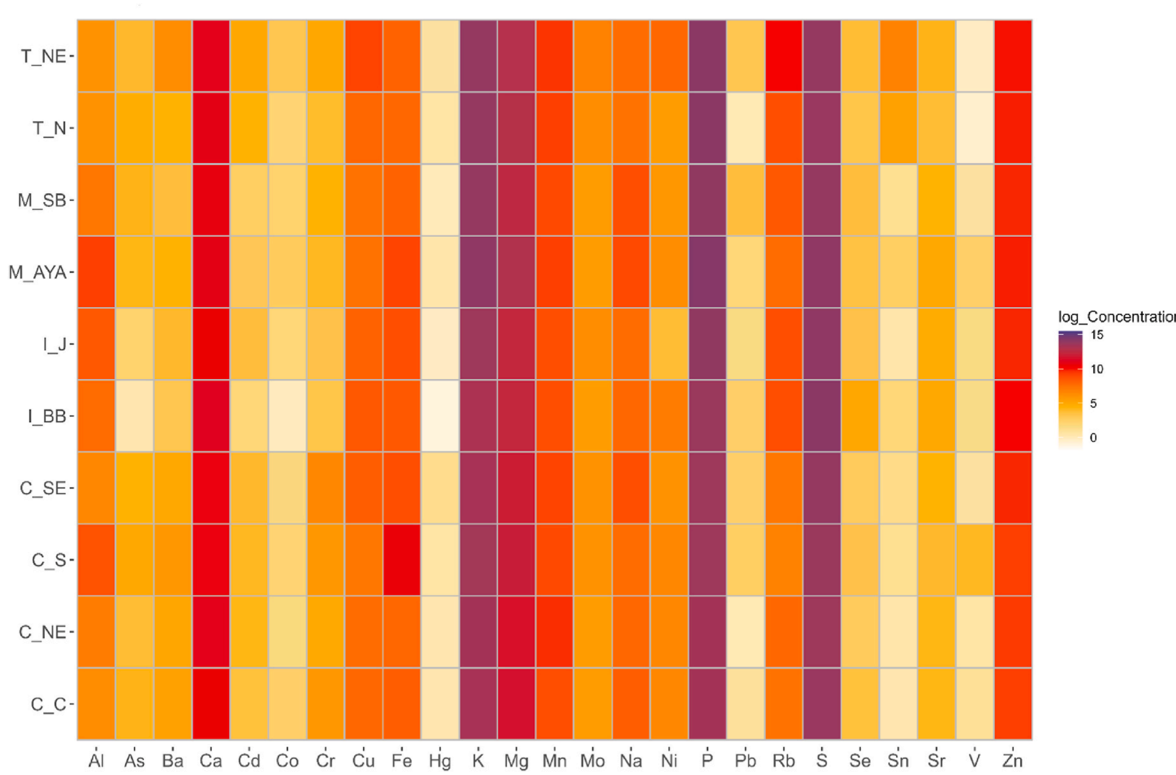


**Fig. 4.** Heatmap of the 25 elemental concentrations (logarithmic form) in different regions of the four countries (irrespective of year). Colors range from white (lowest concentration) to dark purple (highest concentration). Thailand: Northeast (T_NE), North (T_N). Myanmar: ShweBo (M_SB), Ayeyarwady (M_AYA). Indonesia: Java (I_J), Bangka Belitung (I_BB). China: Southeast (C_SE), South (C_S), Northeast (C_NE), Central (C_C). (For interpretation of the references to colour in this figure legend, the reader is referred to the Web version of this article.)

application of an OPLS-DA model because the first orthogonal component was already not significant to the model. So, a PLS-DA model was applied. One predictive and one orthogonal component were selected for Indonesian samples (Figure A3, top left plot); one predictive and two orthogonal components were selected for Myanmar samples (Fig. 5, top left plot); and two predictive components were selected for Thai samples (Fig. 6, top left plot). Each model was presented with 4 plots. A model overview plot that shows the inertia captured by the number of selected components results of cross-validation on the training set. All 3 models showed high inertia captured by the first two predictive components in the case of PLS-DA and by the first predictive and consecutive orthogonal components in the case of OPLS-DA models. This was also reflected in the very good goodness-of-fit (between 0.79 and 0.92) and predictability (between 0.75 and 0.84) parameters observed for all the models. The RMSEE values in the three models were presented below the score plot of each model. They all ranged between 0.14 and 0.2 indicating that the predictions on the samples from the training set was very good. Permutation testing showed that all the models were not overfitted. The score plots showed an excellent separation of the training samples in all the models. The observation diagnostics plots showed that some samples showed good leverage (samples with high score distance within the plane) and some with high orthogonal distance (orthogonal distance between the sample and its projection in the new system of coordinates). No samples fell in the second quarter of the plot so the statistical results along with a re-inspection of analytical data disclosed no formal outliers. Excellent accuracy values (Myanmar - 94,1%, Thailand - 96.9%, and Indonesia - 100%) were obtained for the separate test set of samples of each of the models. The confusion matrices of each model are presented in Table A2. The VIP scores from each of the models are presented in Table A3 (VIP>1), with a summary shown in Table A4. It could be observed that Zn and Ni were selected as geographically discriminant for the 3 countries, along with $\delta^2$H and $\delta^{18}$O. Of all the stable isotopes, $\delta^{18}$O showed the highest VIP score in all the models, followed by $\delta^2$H, confirming their strong relationship with the climatic conditions that influence the rice varieties in different geographic regions. Some elements were selected for two out of the three countries such as Mg, Co, and P, whereas another set of elements was selected for only one country such as Fe, Pb, Hg, Rb, Cd, Se, Cu, Sn, Ba, S, K, Ca, and Mn. All the stable isotopes were selected for Thai rice varieties. However, $\delta^{18}$O and $\delta^{13}$C showed the highest VIP scores, followed by $\delta^{34}$S and $\delta^2$H. This confirmed that $\delta^{18}$O was still the most important stable isotope in terms of discrimination of Asian rice varieties.

## 4. Conclusions

Clear discrimination of the premium rice-producing areas of Thailand, Myanmar and Indonesia was achieved by stable isotope ratio and multi-elemental analysis. IRMS proved to be a valuable tool in this geographic authentication study, with $\delta^{18}$O being the most robust variable, as it was the only one, among 25 elements and 5 isotopes, able to discriminate the premium samples in all three countries. Moreover, ICP-MS results showcased that the micro-elements exhibited higher discriminating potential compared to macro-elements. Differences were also noted in the rice samples originating from China, with all isotopes ($\delta^{13}$C, $\delta^2$H, $\delta^{15}$N, $\delta^{18}$O and $\delta^{34}$S) able to separate the south from the southeastern samples, and Al, Fe and Mg able to characterise the central regions. Considering the very satisfactory (O)PLS-DA accuracy (90–100%) values obtained following LLDF, it is concluded that the combination of the two analytical techniques can correctly classify the premium Asian rice varieties ShweBo Paw San, Thai Jasmine rice, and the Indonesian Ciherang and Inpari. Lastly, inter-annual differences were prominent in the Thai samples, thus highlighting the importance of the sample collection year as a parameter in food authentication studies and traceability databases.

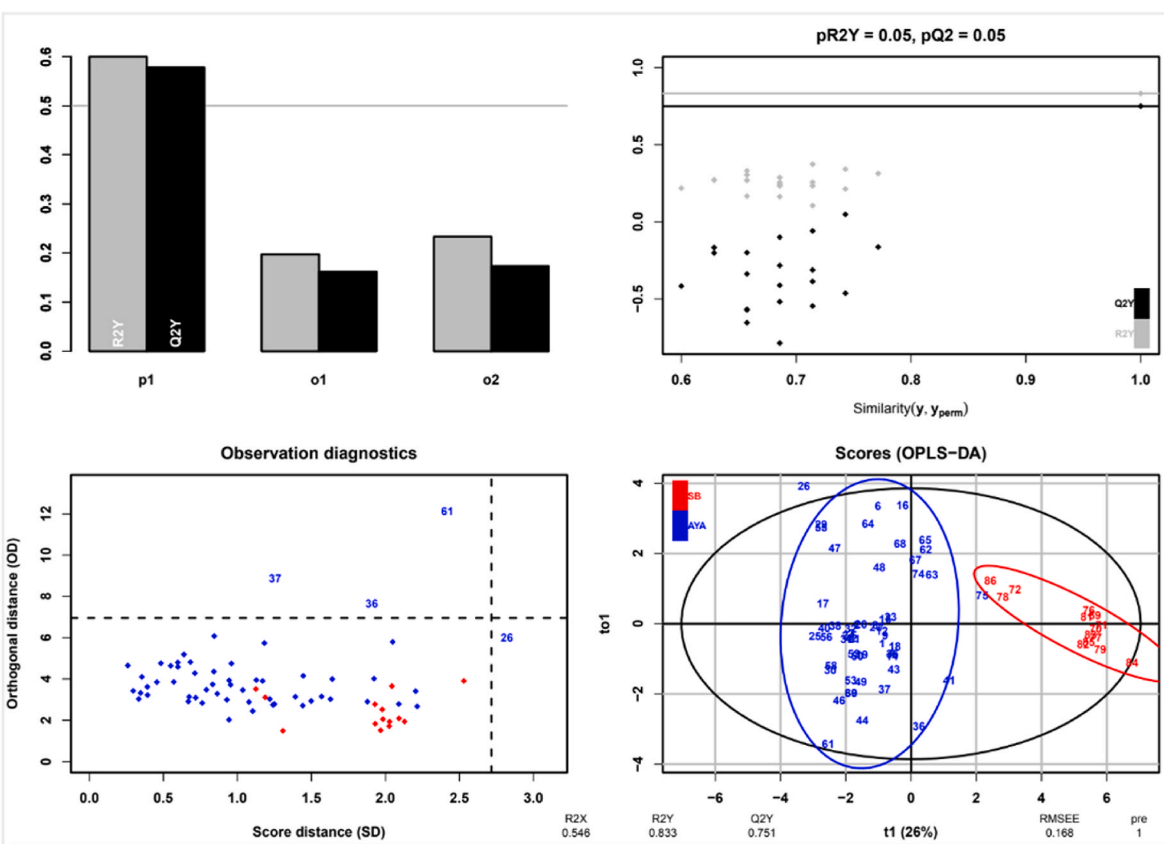


**Fig. 5.** OPLS-DA results of the geographical discrimination of Myanmar rice varieties. Ayeyarwady (AYA) (blue); ShweBo (SB) (red). Top left: Inertia plot (bar plot); Top right: Permutation test; Bottom left: Observation diagnostics test; Bottom right: Score plot. (For interpretation of the references to colour in this figure legend, the reader is referred to the Web version of this article.)

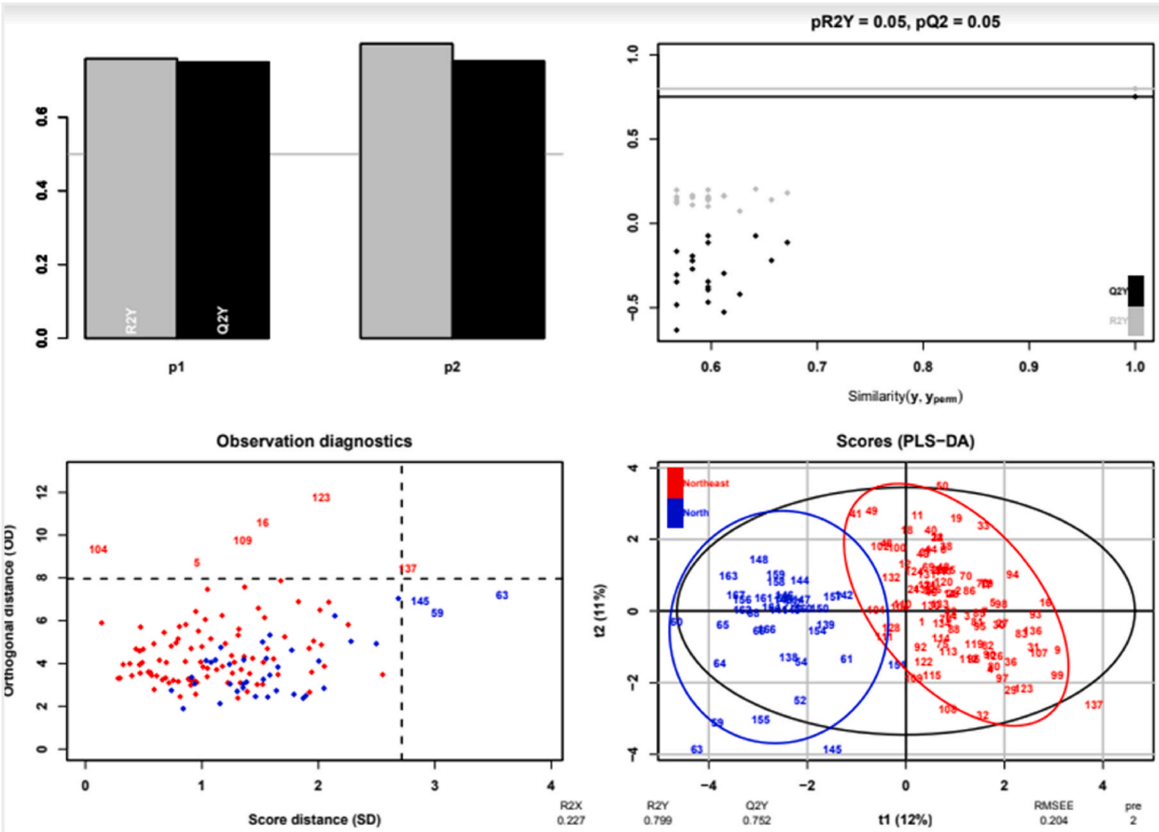


**Fig. 6.** PLS-DA results of the geographical discrimination of Thai rice varieties. North (2018 & 2019) (blue); Northeast (2018 & 2019) (red). Top left: Inertia plot (bar plot); Top right: Permutation test; Bottom left: Observation diagnostics test; Bottom right: Score plot. (For interpretation of the references to colour in this figure legend, the reader is referred to the Web version of this article.)

## CRediT authorship contribution statement

**Zoe Giannioti:** Writing – review & editing, Writing – original draft, Visualization, Validation, Software, Methodology, Investigation, Formal analysis. **Federico Ivan Brigante:** Writing – review & editing, Writing – original draft, Visualization, Software, Methodology. **Simon Kelly:** Writing – review & editing, Resources, Project administration, Conceptualization. **Nives Ogrinc:** Writing – review & editing, Supervision, Resources, Project administration, Funding acquisition. **Marta Jagodic Hudobivnik:** Writing – review & editing, Methodology, Investigation, Data curation. **Darja Mazej:** Writing – review & editing, Supervision, Project administration, Methodology. **Agostino Tonon:** Validation, Methodology, Investigation, Data curation. **Luca Ziller:** Validation, Methodology, Investigation, Data curation. **Chunyapuk Kukusamude:** Writing – review & editing, Resources, Project administration. **Supalak Kongsri:** Writing – review & editing, Resources, Project administration. **Saw Thantar:** Writing – review & editing, Resources, Project administration. **Henni Widyastuti:** Writing – review & editing, Resources, Project administration. **Yuwei Yuan:** Writing – review & editing, Resources, Project administration. **Luana Bontempo:** Writing – review & editing, Writing – original draft, Supervision, Resources, Project administration, Funding acquisition, Conceptualization.

## Declaration of competing interest

The authors declare that they have no known competing financial interests or personal relationships that could have appeared to influence the work reported in this paper.

## Data availability

Data will be made available on request.

## Acknowledgements

Samples were collected as a part of an FAO/IAEA Joint Centre funded Coordinated research Project D52042: “Implementation of Nuclear Techniques for Authentication of Foods with High-Value Labelling Claims (INTACT Food)”.

This research was funded by the European Union’s Horizon 2020 research and innovation programme under the Marie Sklodowska-Curie grant, agreement no. 956265. FoodTraNet.

This study was carried out within the ONFoods - Research and innovation network on food and nutrition Sustainability, Safety and Security - Working ON Foods and received funding from the European Union NextGenerationEU (Piano Nazionale di Ripresa e Resilienza, Missione 4 Componente 2 - Investimento 1.3 – D.D. 1550 11/10/2022, PE00000003).

This manuscript reflects only the authors’ views and opinions, neither the European Union nor the European Commission can be considered responsible for them.

## APPENDIX

**Table A1**
CRMs and Limits of detection (LODs) of the 25 elements analysed by ICP-MS

| Elements | Na | Mg | Al | P | S | K | Ca | V | Cr | Mn | Fe | Co | Ni | Cu | Zn | As | Se | Rb | Sr | Mo | Cd | Sn | Ba | Hg | Pb |
|---|---|---|---|---|---|---|---|---|---|---|---|---|---|---|---|---|---|---|---|---|---|---|---|---|---|
| LOD sample (ng/g) | 150 | 180 | 60 | 350 | 30000 | 420 | 800 | 0.04 | 4.5 | 2.5 | 30 | 0.06 | 4 | 1.5 | 60 | 0.25 | 0.6 | 1.0 | 0.5 | 0.2 | 0.1 | 0.4 | 0.5 | 0.1 | 0.2 |
| Rice flour 1568b: | | | | | | | | | | | | | | | | | | | | | | | | | |
| Reference value (ng/g) | 6740 | 559000 | 4210 | 1530000 | 1200000 | 1282000 | 118400 | | | 19200 | 7420 | 18 | | 2350 | 19420 | 285 | 365 | 6198 | | 1451 | 22 | 5.0 | | 5.91 | 8.0 |
| Uncertainty of reference value | 190 | 10000 | 340 | 40000 | 10000 | 11000 | 3100 | | | 1800 | 440 | 1 | | 160 | 260 | 14 | 29 | 26 | | 48 | 1 | 1.0 | | 0.36 | 3.0 |
| Measured value - average (ng/g) | 6426 | 517880 | 3985 | 1536368 | 1210152 | 1238728 | 120482 | 4.4 | 31.8 | 19016 | 7010 | 19 | 209,8 | 2312 | 18762 | 285 | 365 | 5901 | 131,9 | 1430 | 21 | 5.0 | 114.0 | 5.91 | 7.4 |
| Measured value - rsd (%) | 10.5 | 11.6 | 3.8 | 6.5 | 5.7 | 9.2 | 11.9 | 9.6 | 4.3 | 8,2 | 9,8 | 7,2 | 4,1 | 6,4 | 8,3 | 6,0 | 6,3 | 7,6 | 6,6 | 8,5 | 9,7 | 14.8 | 8.1 | 10.3 | 5.0 |
| Durum wheat flour 8436: | | | | | | | | | | | | | | | | | | | | | | | | | |
| Reference value (ng/g) | 16000 | 1070000 | 11700 | 2900000 | 1930000 | 3180000 | 278000 | 21 | 23 | 16000 | 41500 | 8.0 | 170 | 4300 | 22200 | | | 2000 | 1190 | 700 | 110 | | 2110 | | 23 |
| Uncertainty of reference value | 6100 | 80000 | 4700 | 220000 | 280000 | 140000 | 26000 | 6 | 9 | 1000 | 4000 | 4,0 | 80 | 690 | 1700 | | | 400 | 90 | 120 | 50 | | 470 | | 6 |
| Measured value - average (ng/g) | 16746 | 1148710 | 12325 | 2887931 | 1913673 | 3287337 | 273112 | 21.0 | 23.0 | 16154 | 43792 | 7.2 | 170 | 4370 | 22953 | | | 2096 | 1190 | 710 | 116 | | 2110 | | 24.8 |
| Measured value - rsd (%) | 7.37 | 9.89 | 1.38 | 6.52 | 6.58 | 7.84 | 10.72 | 13.44 | 3.72 | 6.77 | 8.90 | 7.98 | 4.71 | 3.93 | 7.07 | | | 6.47 | 5.68 | 4.02 | 7.07 | | 6.46 | | 3.47 |
| Repeatability | 9 | 6 | 8 | 4.5 | 4 | 5 | 5 | 9 | 11 | 6 | 7 | 6 | 8 | 8 | 5 | 5 | 8 | 5 | 7 | 5 | 8 | 18 | 6 | 6 | 11 |

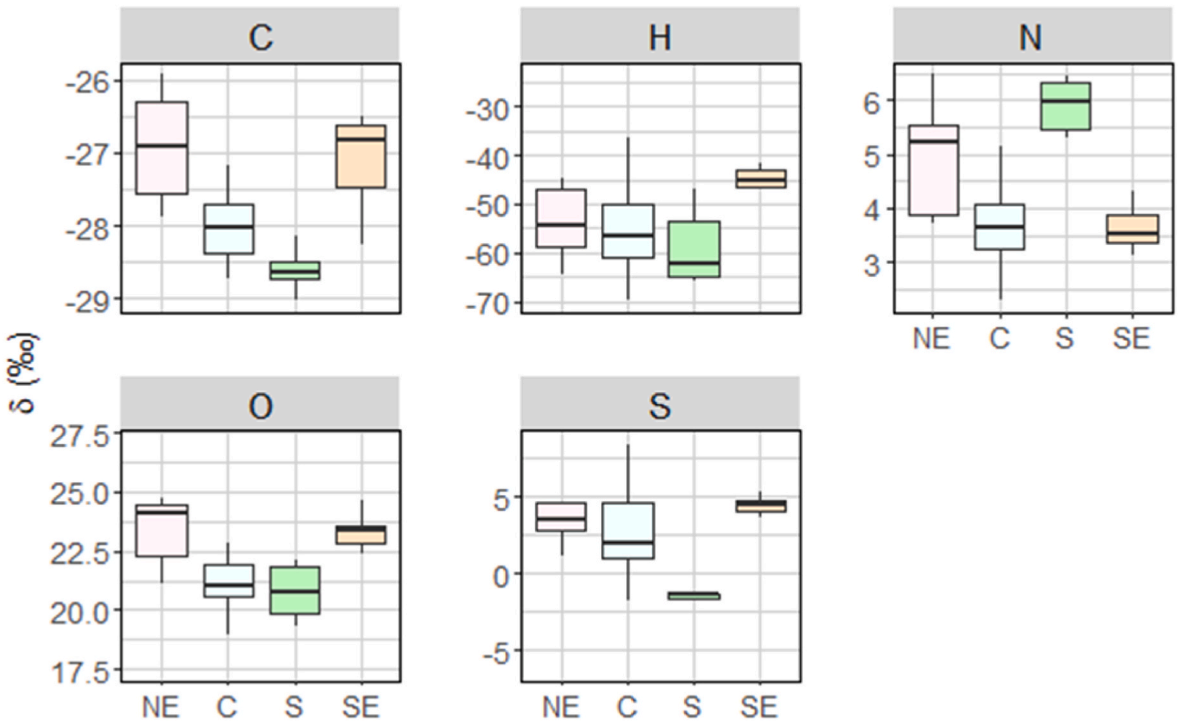


**Fig. A1.** Discrimination between Chinese rice from the Northeast (NE: HLJ, JL, LN), Central (C: HB, HN, JX, AH), Southern (S: GZ) and Southeastern (SE: ZJ, JS) regions, based on $\delta^{13}C$, $\delta^{2}H$, $\delta^{15}N$, $\delta^{18}O$ and $\delta^{34}S$ values.

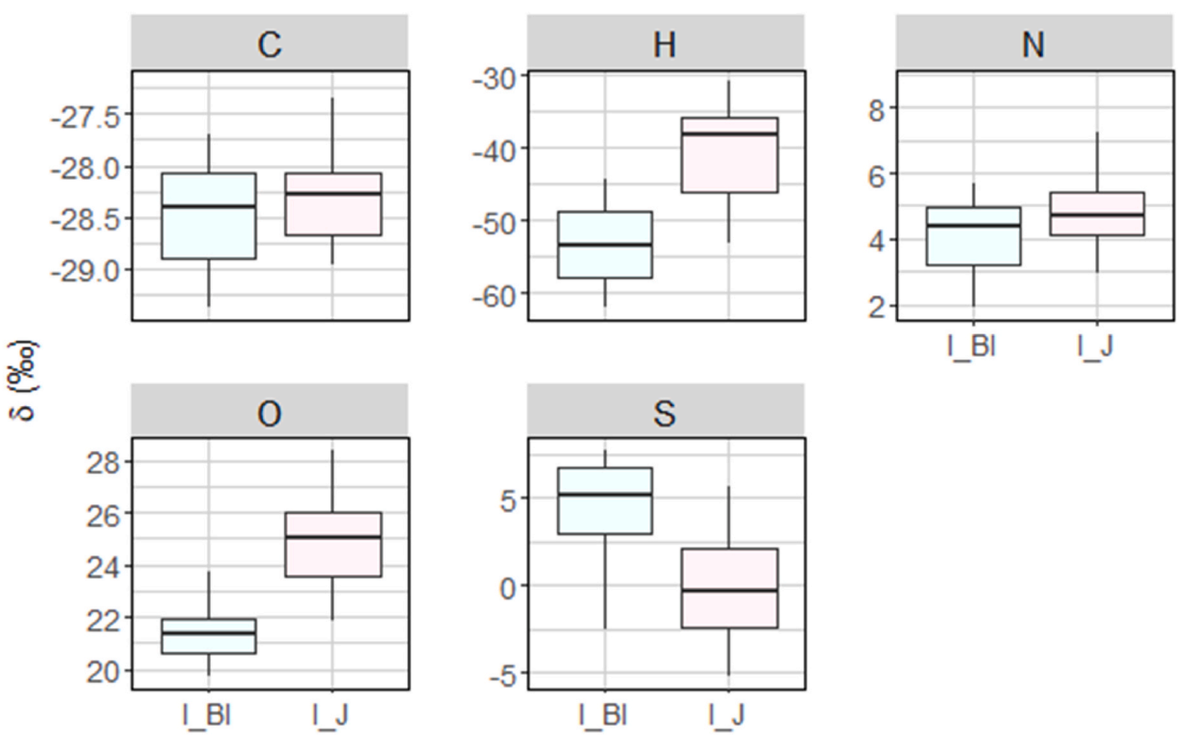


**Fig. A2.** Discrimination between Indonesian rice from Bangka Belitung Islands (I_Bl) and Java (I_J), based on $\delta^{13}C$, $\delta^{2}H$, $\delta^{15}N$, $\delta^{18}O$ and $\delta^{34}S$ values.

**Table A2**
Confusion matrices of the (O)PLS-DA models.

| (A) Indonesia | | |
|---|---|---|
| | Bangka Belitung | Java |
| Bangka Belitung | 4 | 0 |
| Java | 0 | 4 |
| (B) Myanmar | | |
| | Ayeyarwady | ShweBo |
| Ayeyarwady | 14 | 1 |
| ShweBo | 0 | 2 |
| (C) Thailand | | |
| | North | Northeast |
| North | 9 | 1 |
| Northeast | 0 | 23 |

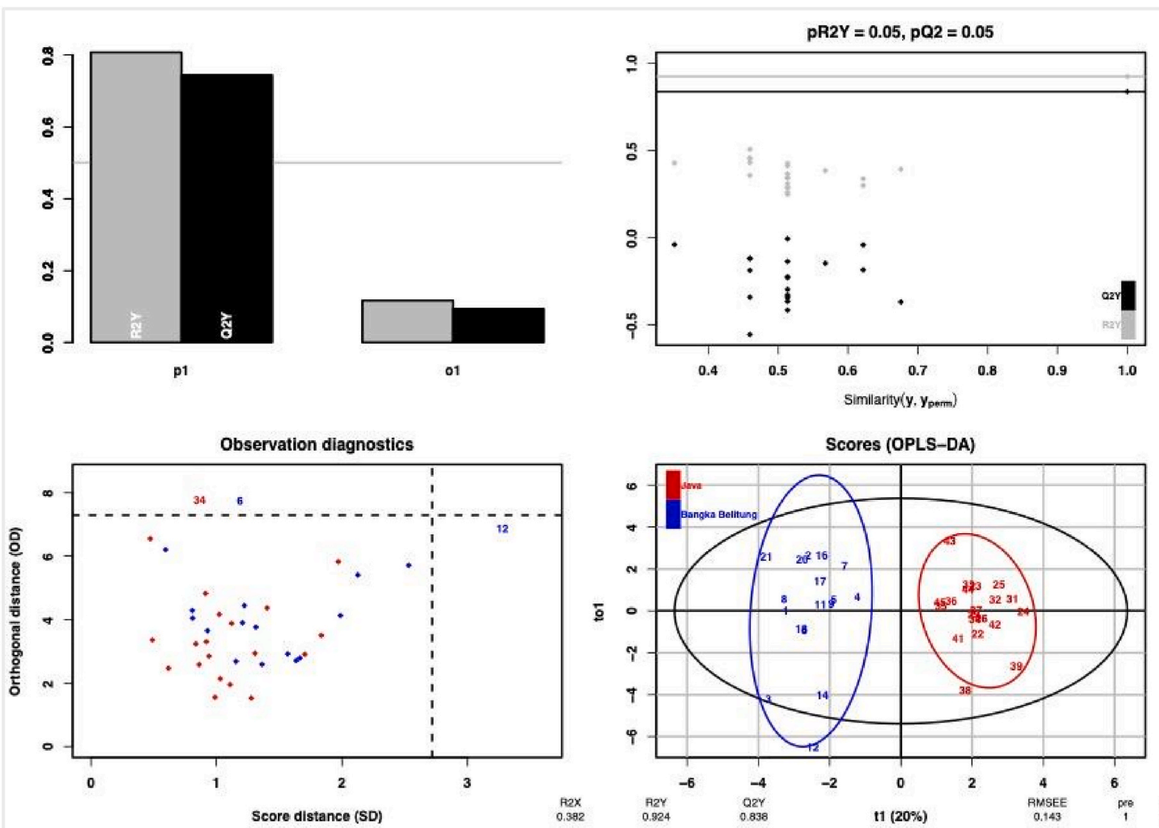


**Fig. A3.** OPLS-DA results of the geographical discrimination of Indonesian rice varieties. Bangka Belitung (blue); Java (red). Top left: Inertia plot (bar plot); Top right: permutation test; Bottom left: observation diagnostics test; Bottom right: score plot.

**Table A3**
Variable selection results of the (O)PLS-DA models (VIP>1).

| (A) Indonesia - Bangka Belitung vs Java | |
|---|---|
| Variable | VIP |
| $\delta^{18}O$ | 1.697 |
| $\delta^{2}H$ | 1.669 |
| $\delta^{34}S$ | 1.668 |
| Co | 1.544 |
| Rb | 1.526 |
| Zn | 1.373 |
| Mg | 1.371 |
| Cd | 1.32 |
| Ni | 1.236 |
| Ca | 1.225 |
| Se | 1.143 |

(*continued on next page*)

**Table A3** (*continued*)

| Variable | VIP |
|---|---|
| **(A) Indonesia - Bangka Belitung vs Java** | |
| Sn | 1.061 |
| P | 1.058 |
| S | 1.016 |
| **(B) Myanmar - Paw San ShweBo vs Ayeyarwady** | |
| Variable | VIP |
| $\delta^{18}$O | 1.67 |
| Zn | 1.586 |
| $\delta^{2}$H | 1.486 |
| Cu | 1.476 |
| Mn | 1.27 |
| K | 1.243 |
| Mg | 1.238 |
| P | 1.183 |
| Pb | 1.129 |
| $\delta^{15}$N | 1.089 |
| Ni | 1.074 |
| Fe | 1.049 |
| Hg | 1.033 |
| **(C) Thailand - Jasmine rice - North vs Northeast** | |
| Variable | VIP |
| $\delta^{18}$O | 2.402 |
| $\delta^{13}$C | 2.366 |
| Ba | 1.582 |
| $\delta^{34}$S | 1.46 |
| Zn | 1.422 |
| $\delta^{2}$H | 1.369 |
| Co | 1.196 |
| Ni | 1.095 |
| $\delta^{15}$N | 1.024 |

**Table A4**
Summary of (O)PLS-DA discriminant variables with VIP>1.4 for the models (denoted in grey).

| VIP>1.4 | $\delta^{13}$C | $\delta^{18}$O | $\delta^{2}$H | $\delta^{34}$S | Co | Rb | Cu | Ba | Zn |
|---|---|---|---|---|---|---|---|---|---|
| Thailand | ■ | ■ | | ■ | | | | ■ | ■ |
| Myanmar | | ■ | ■ | | | | ■ | | ■ |
| Indonesia | | ■ | ■ | ■ | ■ | ■ | | | |

## References


Anderson, K. A., & Smith, B. W. (2006). Effect of season and variety on the differentiation of geographic growing origin of pistachios by stable isotope profiling. *Journal of Agricultural and Food Chemistry, 54*(5), 1747–1752. https://doi.org/10.1021/jf052928m

Antriyandarti, E., Agustono, Ani, S. W., Rusdiyana, E., & Sukaton, D. L. (2023). Consumers' willingness to pay for local rice: Empirical evidence from Central Java, Indonesia. *Journal of Agriculture and Food Research, 14*, Article 100851. https://doi.org/10.1016/j.jafr.2023.100851

Arif, M., Chilvers, G., Day, S., Naveed, S. A., Woolfe, M., Rodionova, O. Y., et al. (2021). Differentiating Pakistani long-grain rice grown inside and outside the accepted Basmati Himalayan geographical region using a 'one-class' multi-element chemometric model. *Food Control, 123*, Article 107827. https://doi.org/10.1016/j.foodcont.2020.107827

Aye, H. N., Khaing, A. A., Tun, P. T., Htun, T. M., & Win, K. K. (2019). Grain quality of paw san varieties from Pathein, pyapon and Shwebo townships. *Journal of Agricultural Research, 6*(2), 111–118.

Azcarate, S. M., Ríos-Reina, R., Amigo, J. M., & Goicoechea, H. C. (2021b). Data handling in data fusion: Methodologies and applications. *TrAC, Trends in Analytical Chemistry, 143*, Article 116355. https://doi.org/10.1016/j.trac.2021.116355

Badia-Melis, R., Mishra, P., & Ruiz-García, L. (2015). Food traceability: New trends and recent advances. A review. *Food Control, 57*, 393–401. https://doi.org/10.1016/j.foodcont.2015.05.005

Bateman, A. S., Kelly, S. D., & Jickells, T. D. (2005). Nitrogen isotope relationships between crops and fertilizer: Implications for using nitrogen isotope analysis as an indicator of agricultural regime. *Journal of Agricultural and Food Chemistry, 53*(14), 5760–5765. https://doi.org/10.1021/jf050374h

Boonkong, A., Jiang, B., Kassoh, F. S., & Srisukwatanachai, T. (2023). Chinese and Thai consumers' willingness to pay for quality rice attributes: A discrete choice experiment method. *Frontiers in Sustainable Food Systems, 7*. https://doi.org/10.3389/fsufs.2023.1270331

Callao, M. P., & Ruisánchez, I. (2018). An overview of multivariate qualitative methods for food fraud detection. *Food Control, 86*, 283–293. https://doi.org/10.1016/j.foodcont.2017.11.034

Camin, F., Bontempo, L., Heinrich, K., Horacek, M., Kelly, S. D., Schlicht, C., et al. (2007). Multi-element (H,C,N,s) stable isotope characteristics of lamb meat from different European regions. *Analytical and Bioanalytical Chemistry, 389*(1), 309–320. https://doi.org/10.1007/s00216-007-1302-3

Campanelli, G., Amenta, M., Bontempo, L., Leteo, F., Montemurro, F., Platani, C., et al. (2024). Innovative tools for nitrogen fertilization traceability in organic farming products: A cauliflower case study. *Horticulturae, 10*(1), 94. https://doi.org/10.3390/horticulturae10010094

Cheajesadagul, P., Arnaudguilhem, C., Shiowatana, J., Siripinyanond, A., & Szpunar, J. (2013). Discrimination of geographical origin of rice based on multi-element fingerprinting by high resolution inductively coupled plasma mass spectrometry. *Food Chemistry, 141*(4), 3504–3509. https://doi.org/10.1016/j.foodchem.2013.06.060

Chung, I.-M., Kim, J.-K., Lee, K.-J., Park, S.-K., Lee, J.-H., Son, N.-Y., et al. (2018). Geographic authentication of Asian rice (Oryza sativa L.) using multi-elemental and stable isotopic data combined with multivariate analysis. *Food Chemistry, 240*, 840–849. https://doi.org/10.1016/j.foodchem.2017.08.023

Chutsagulprom, N., Chaisee, K., Wongsaijai, B., Inkeaw, P., & Oonariya, C. (2022). Spatial interpolation methods for estimating monthly rainfall distribution in Thailand. *Theoretical and Applied Climatology, 148*(1–2), 317–328. https://doi.org/10.1007/s00704-022-03927-7

Codex Alimentarius (Codex). (1995). General standard for contaminants and toxins in food and feed (Codex stan 193–1995). Available on https://knowledge4policy.ec.europa.eu/publication/general-standard-contaminants-toxins-food-feed-codex-stan-193-1995_en. (Accessed 7 May 2024).

?European Union Intellectual Property Office (EUIPO). (2019). Geographical indications in the asean region: A booklet on asean geographical indications procedure and products. Bangkok: EUIPO, Arise + ASEAN Intellectual Property Rights. pp. 74-75. https://internationalipcooperation.eu/sites/default/files/arise-docs/2019/ASEAN_GI-Booklet.pdf.

Galindo-Prieto, B., Eriksson, L., & Trygg, J. (2014). Variable influence on projection (VIP) for orthogonal projections to latent structures (OPLS). *Journal of Chemometrics, 28*, 623–632. https://doi.org/10.1002/cem.2627

Hubert, M., Rousseeuw, P. J., & Vanden Branden, K. (2005). ROBPCA—a new approach to robust principal component analysis. *Technometrics, 147*, 64–79.

Islam, R., & Khan, M. M. (2019). *The science of climate change*. John Wiley & Sons. ISBN 1119522846, 9781119522843.

Japan International Cooperation Agency (JICA). (2013). *The republic of the union of Myanmar. Data collection Survey on coal fired thermal power generation* (p. 30) (report).

Körner, C., Farquhar, G. D., & Roksandic, Z. (1988). A global survey of carbon isotope discrimination in plants from high altitude. *Oecologia, 74*(4), 623–632. https://doi.org/10.1007/bf00380063

Kukusamude, C., & Kongsri, S. (2018). Elemental and isotopic profiling of Thai jasmine rice (Khao Dawk Mali 105) for discrimination of geographical origins in Thung Kula Rong Hai area, Thailand. *Food Control, 91*, 357–364. https://doi.org/10.1016/j.foodcont.2018.04.018

Li, A., Keely, B., Chan, S. H., Baxter, M., Rees, G., & Kelly, S. (2015). Verifying the provenance of rice using stable isotope ratio and multi-element analyses: A feasibility study. *Quality Assurance and Safety of Crops & Foods, 7*(3), 343–354. https://doi.org/10.3920/qas2013.0378

Li, C., Nie, J., Zhang, Y., Shao, S., Liu, Z., Rogers, K. M., et al. (2022). Geographical origin modeling of Chinese rice using stable isotopes and trace elements. *Food Control, 138*, Article 108997. https://doi.org/10.1016/j.foodcont.2022.108997

Li, C., Wang, Q., Shao, S., Chen, Z., Nie, J., Liu, Z., et al. (2021). Stable isotope effects of biogas slurry applied as an organic fertilizer to rice, straw, and Soil. *Journal of Agricultural and Food Chemistry, 69*(29), 8090–8097. https://doi.org/10.1021/acs.jafc.1c01740

Liu, Z., Zhang, W., Zhang, Y., Chen, T., Shao, S., Zhou, L., et al. (2019). Assuring food safety and traceability of polished rice from different production regions in China and Southeast Asia using chemometric models. *Food Control, 99*, 1–10. https://doi.org/10.1016/j.foodcont.2018.12.011

Mustikarini, E. D., Prayoga, G. I., Santi, R., & Sari, N. P. (2021). Advanced yield trial of F7 upland rice lines with lodging resistance in Bangka regency, Bangka Belitung islands province, Indonesia. *IOP Conference Series: Earth and Environmental Science, 926*(1), Article 012022. https://doi.org/10.1088/1755-1315/926/1/012022

Myint, P. L., & Napasintuwong, O. (2015). Cost and return comparison between paw san rice and non-paw san rice production in Myanmar. *PSAKU International Journal of Interdisciplinary Research, 4*(2), 77–85. https://doi.org/10.12778/235108618x15452373185453

Nurtjahya, E., Nur, M. M., & Mulyono, E. (2009). Rice field cultivation on tin-mined land in Bangka Island, Indonesia. In A. Fourie, & M. Tibbet (Eds.), *Mine closure 2009: Proceedings of the fourth international seminar on mine closure* (pp. 549–560).

Oo, K. T., Haishan, C., & Jonah, K. (2023). Climate change impact on the trigger of natural disasters over south-eastern himalayas foothill region of Myanmar: Extreme rainfall analysis. *International Journal of Geophysics, 2186857*. https://doi.org/10.1155/2023/2186857

Oo, K. S., Kongjaimun, A., Khanthong, S., Yi, M., Myint, T. T., Korinsak, S., et al. (2015). Characterization of Myanmar paw San Hmwe accessions using functional genetic markers. *Rice Science, 22*(2), 53–64. https://doi.org/10.1016/j.rsci.2015.05.004

Philibosian, B., & Simons, M. (2011). A survey of volcanic deformation on Java using ALOS PALSAR interferometric time series. *Geochemistry, Geophysics, Geosystems, 12*(11). https://doi.org/10.1029/2011gc003775

Quinn, B., McCarron, P., Hong, Y., Birse, N., Wu, D., Elliott, C. T., et al. (2022). Elementomics combined with DD-simca and K-NN to identify the geographical origin of rice samples from China, India, and Vietnam. *Food Chemistry, 386*, Article 132738. https://doi.org/10.1016/j.foodchem.2022.132738

Rodiouchkina, K., Rodushkin, I., Goderis, S., & Vanhaecke, F. (2022). A comprehensive evaluation of sulfur isotopic analysis (δ34S and δ33S) using multi-collector ICP-MS with characterization of reference materials of geological and biological origin. *Analytica Chimica Acta, 340744*. https://doi.org/10.1016/j.aca.2022.340744

Sasmita, P., & Nugraha, Y. (2020). Rice breeding strategy for climate resilience and ValueAddition in Indonesia. In P. Lestari, K. Mulya, D. W. Utami, D. Satyawan, & M. Supriadi (Eds.), *Strategies and technologies for the utilization and improvement of rice* (pp. 67–82). IAARD PRESS. ISBN: 978-602-344-309-3.

Shahbandeh, M. (2024). *Rice production worldwide by country 2023*. Statista. https://www.statista.com/statistics/255945/top-countries-of-destination-for-us-rice-exports-2011/.

Sheng, M., Zhang, W., Nie, J., Li, C., Zhu, A.-X., Hu, H., et al. (2022). Predicting isoscapes based on an environmental similarity model for the geographical origin of Chinese rice. *Food Chemistry, 397*, Article 133744. https://doi.org/10.1016/j.foodchem.2022.133744

Sitaresmi, T., Hairmansis, A., Widyastuti, Y., Rachmawati, Susanto, U., Wibowo, B. P., et al. (2023). Advances in the development of rice varieties with better nutritional quality in Indonesia. *Journal of Agriculture and Food Research, 12*, Article 100602. https://doi.org/10.1016/j.jafr.2023.100602

Sitaresmi, T., Safitri, H., Nafisah, Susanto, U., Hairmansis, A., Gunarsih, C., et al. (2023). Selection of rice promising lines having ciherang's idiotype for improved resistance of main pest and diseases. *IOP Conference Series: Earth and Environmental Science, 1172*(1), Article 012022. https://doi.org/10.1088/1755-1315/1172/1/012022

Smilde, A. K., & Van Mechelen, I. (2019). A framework for low-level data fusion. *Data Handling in Science and Technology, 31*, 27–50. https://doi.org/10.1016/b978-0-444-63984-4.00002-8

Suchecki Barnet, L., Harumi Yamashita, G., Anzanello, M. J., & Pozebon, D. (2023). Determination of the most informative chemical elements for discrimination of rice samples according to the producing region. *Food Chemistry, 402*, Article 134208. https://doi.org/10.1016/j.foodchem.2022.134208

Sukarman, S., Gani, R. A., & Asmarhansyah, A. (2020). Tin mining process and its effects on soils in Bangka Belitung islands province, Indonesia. *SAINS TANAH - Journal of Soil Science and Agroclimatology, 17*(2), 180. https://doi.org/10.20961/stjssa.v17i2.37606

Thantar, S., Mihailova, A., Islam, M. D., Maxwell, F., Hamed, I., Vlachou, C., et al. (2024). Geographical discrimination of Paw San Rice cultivated in different regions of Myanmar using near-infrared spectroscopy, headspace-gas chromatography-ion mobility spectrometry and Chemometrics. *Talanta, 273*, Article 125910. https://doi.org/10.1016/j.talanta.2024.125910

Thein, M. S. (2015). Marginal land vs productive land: A case study on cultivating Myanmar local quality rice (oryza sativa L) morphotypes. In *International soil conference ISC 2015 "sustainable uses of soil in harmony with food security"*. Thailand: Phetchaburi. Paper presentation.

Thévenot, E. A., Roux, A., Xu, Y., Ezan, E., & Junot, C. (2015). Analysis of the human adult urinary metabolome variations with age, body mass index, and gender by implementing a comprehensive workflow for univariate and OPLS statistical analyses. *Journal of Proteome Research, 14*(8), 3322–3335. https://doi.org/10.1021/acs.jproteome.5b00354

Wadood, S. A., Li, C., Nie, J., Rogers, K. M., Mei, H., Zhang, Y., et al. (2024). Stable isotopic fingerprinting of authentic basmati rice from Pakistan. *Food Control, 110166*. https://doi.org/10.1016/j.foodcont.2023.110166

Wang, J., Chen, T., Zhang, W., Zhao, Y., Yang, S., & Chen, A. (2020). Tracing the geographical origin of rice by stable isotopic analyses combined with chemometrics. *Food Chemistry, 313*, Article 126093. https://doi.org/10.1016/j.foodchem.2019.126093

Wassenaar, L. I., & Hobson, K. A. (2003). Comparative equilibration and online technique for determination of non-exchangeable hydrogen of keratins for use in animal migration studies. *Isotopes in Environmental and Health Studies, 39*(3), 211–217. https://doi.org/10.1080/1025601031000096781

Wulandari, D., Agus, C., Rosita, R., Mansur, I., & Fikri Maulana, A. (2022). Impact of tin mining on soil physio-chemical properties in Bangka, Indonesia. *Jurnal Sains & Teknologi Lingkungan, 14*(2), 114–121. https://doi.org/10.20885/jstl.vol14.iss2.art2

Zhao, H., Wang, F., & Yang, Q. (2020). Origin traceability of peanut kernels based on multi-element fingerprinting combined with multivariate data analysis. *Journal of the Science of Food and Agriculture, 100*(10), 4040–4048. https://doi.org/10.1002/jsfa.10449

Zhi, L., Yuan, W., Yudi, H., Weixing, Z., Ming, M., Wei, L., et al. (2023). Multi-stable isotope and multi-element origin traceability of rice from the main producing regions in Asia: A long-term investigation during 2017-2020. *Food Chemistry, 135417*. https://doi.org/10.1016/j.foodchem.2023.135417